Mon. Not. R. Astron. Soc. **358,** 202–210 (2005) doi:10.1111/j.1365-2966.2005.08803.x

Neutral hydrogen gas in interacting galaxies: the NGC 1511 galaxy group

Bärbel Koribalski[1]★ and Eva Manthey[2]

[1]*Australia Telescope National Facility, CSIRO, PO Box 76, Epping, NSW 1710, Australia*
[2]*University of Bochum, Department of Astronomy, 44780 Bochum, Germany*

Accepted 2005 January 2. Received 2004 December 17; in original form 2004 November 5

ABSTRACT

We present H I line and 20-cm radio continuum observations of the NGC 1511 galaxy group obtained with the Australia Telescope Compact Array. The data reveal an extended, rather disturbed H I distribution for the peculiar starburst galaxy NGC 1511 and a narrow bridge to its small companion galaxy, NGC 1511B, which has been severely distorted by the interaction/collision between the two galaxies. No stellar counterpart to the gaseous bridge has been detected. In addition, we find that the peculiar optical ridge to the east of NGC 1511 is probably the stellar remnant of a galaxy completely disrupted by interactions with NGC 1511. The slightly more distant neighbour, NGC 1511A, shows a regular H I velocity field and no obvious signs of interactions.

Radio continuum emission from NGC 1511 reveals three prominent sources on top of a more diffuse, extended distribution. We derive an overall star formation rate of $7\,M_\odot\,yr^{-1}$. The most enhanced star formation is found in the south-eastern part of the disc, coincident with several bright H II regions, and closest to the peculiar optical ridge. No continuum emission was detected in the companions, but NGC 1511B appears to show an H II region at its faint western edge, closest to NGC 1511. The group displays a prime example of interaction-induced star formation activity.

Key words: galaxies: individual NGC 1511 – galaxies: individual: NGC 1511A – galaxies: individual: NGC 1511B – galaxies: interactions.

1 INTRODUCTION

Neutral hydrogen gas (H I) is the best tracer for galaxy–galaxy interactions. Because the H I envelope of a galaxy is generally more extended than its stellar disc (Broeils & van Woerden 1994; Salpeter & Hoffman 1996), it is more easily disrupted by tidal forces from neighbouring galaxies. Galaxy pairs and groups often show very complex extended H I distributions, including H I tails and bridges, even if the corresponding optical images show little disturbance. For examples see Irwin (1994), Yun, Ho & Lo (1994), Smith, Struck & Pogge (1997), Koribalski & Dickey (2004) and the H I Rogues Gallery (Hibbard et al. 2001). Here, we use H I line observations to investigate the interaction history and dynamics of the NGC 1511 galaxy group.

The starburst galaxy NGC 1511 is the most prominent member of a compact galaxy triplet at a distance of ∼17.5 Mpc ($H_0 = 75$ km s^{-1} Mpc^{-1}). Its companions, NGC 1511B and 1511A, lie at projected distances of 7.3 arcmin (37 kpc) and 10.7 arcmin (54 kpc), respectively. Table 1 lists some properties for all three galaxies. The stellar disc of NGC 1511 (see, e.g. Sandage & Bedke 1994; Eskridge et al. 2002) contains several bright hotspots, a prominent dust lane and various peculiar extensions. Faint loops and plumes are seen to the north-east of the disc, while the hotspots are located in a peculiar hook at the south-eastern end of the disc, which is best seen in infrared images (Eskridge et al. 2002; Jarrett et al. 2003). In addition, deep optical images reveal an extended vertical ridge ∼1.5 arcmin east of the south-eastern end of the disc, the nature of which we will explore here. Optical short exposures of NGC 1511 show a remarkable resemblance to the peculiar starburst galaxy NGC 1808 (Koribalski et al. 1993). The optical diameter of NGC 1511 (3.5 × 1.2 arcmin^2 or 17.5 × 6.1 kpc) is approximately twice that of the neighbouring galaxies NGC 1511A and B. While NGC 1511A appears slightly inclined and symmetric, NGC 1511B is an extremely thin, edge-on galaxy with a faint extension to the west. There is a hint of an H II region at the westernmost end. The pecularities of both NGC 1511 and 1511B suggest they are interacting. Koribalski (1996) briefly commented on the post-interaction/-merger nature of NGC 1511. The H I distribution of the triplet is also briefly discussed by Nordgren et al. (1997). The star formation history of NGC 1511 can be used to estimate the interaction time-scale. Sekiguchi & Wolstencroft (1993) find that NGC 1511 has an H II region like emission spectrum with high excitation (see also Kewley et al. 2000), suggesting ongoing star formation mixed with a burst ∼10^8–10^9 yr ago. Thornley et al. (2000) find indications of massive star formation ($\gtrsim 50\,M_\odot$) on a short time-scale of $\leqslant 10^7$ yr using mid-infrared

★E-mail: Baerbel.Koribalski@csiro.au

Table 1. Some basic parameters of the observed spiral galaxies.

	NGC 1511	NGC 1511A	NGC 1511B	Ref.
Centre position:				
α(J2000)	$03^h59^m35\overset{s}{.}8$	$04^h00^m19\overset{s}{.}4$	$04^h00^m54\overset{s}{.}6$	(1)
δ(J2000)	$-67^\circ38'07''$	$-67^\circ48'28''$	$-67^\circ36'\,42''$	
Type	SAa pec	SB0	SBd?	(1)
Optical diameter	3.5×1.2 arcmin^2	1.7×0.4 arcmin^2	1.7×0.3 arcmin^2	(1)
Inclination	74 ± 2	75 ± 4	87 ± 4	(6)
Position angle	125°	110°	98°	(1, 2)
($v_{\rm HI}$ km s^{-1})	1351 ± 7	1323 ± 10	1304 ± 3	(1, 3, 6)
$v_{\rm opt}$ (km s^{-1})	1334 ± 48	1358 ± 69	–	(1)
$v_{\rm H\alpha}$(km s^{-1})	1334 ± 10	1291 ± 10	1439 ± 10	(2)
$v_{\rm CO}$ (km s^{-1})	1270 ± 7	–	–	(4)
$F_{\rm HI}$ (Jy km s^{-1})	73.6	20.6	–	(3)
$S_{60\mu m}$ (Jy)	23.67	0.44	–	(5)
$S_{100\mu m}$ (Jy)	37.99	<2.16	–	(5)
B magnitude	12.11	14.23	15.12	(1)
A_B	0.265	0.257	0.236	(7)
L_B (10^9 L$_\odot$)	4.9	0.7	0.3	
L_X (10^{40} erg s^{-1})	1.1	–	–	(8)

References: (1) de Vaucouleurs et al. (1991; RC3); (2) Lauberts (1982; ESO-LV); (3) Mathewson & Ford (1996); (4) Elfhag et al. (1996); (5) Moshir et al. (1990); (6) Nordgren et al. (1997); (7) Schlegel, Finkbeiner & Davis (1998); (8) Dahlem et al. (2003).

spectroscopy. Elfhag et al. (1996) observed the centre of NGC 1511 with the Swedish–ESO Submillimetre Telescope and find a CO intensity of $I_{\rm CO} = 11.5$ K km s^{-1} (adjusted to our adopted distance). This corresponds to a nuclear H_2 mass of 5.5×10^8 M$_\odot$ if we adopt the standard conversion factor of $N_{\rm H_2}/I_{\rm CO} = 2.3 \times 10^{20}$ H$_2$ cm^{-2} (K km s^{-1})$^{-1}$ (Strong et al. 1988). Radio continuum, X-ray and ultraviolet (UV) data were obtained by Dahlem et al. (2001, 2003), while Lehnert & Heckman (1995) presented an Hα image. These data confirm the starburst character of NGC 1511.

The paper is organized as follows. In Section 2, we summarize the observations and data reduction. In Section 3, we present the 20-cm radio continuum results and derive star formation rates (SFRs) for NGC 1511. The H I morphology and kinematics of all members of the NGC 1511 galaxy group are described in Section 4. The overall gas dynamics are discussed in Section 5 and Section 6 contains our conclusions.

2 OBSERVATIONS AND DATA REDUCTION

H I line and 20-cm radio continuum observations of the NGC 1511 galaxy group were obtained with the Australia Telescope Compact Array (ATCA) in 1995 March and August using the 1.5A and 375 arrays. For a summary of the observations, see Table 2.

Data reduction was carried out with the MIRIAD software package using standard procedures. The data were split into a narrow-band radio continuum and an H I line data set using a first-order fit to the line-free channels. The H I channel maps were made using natural (na) and robust ($r = 0$) weighting of the *uv* data in the velocity range from 1050 to 1550 km s^{-1} using steps of 10 km s^{-1}. The resulting synthesized beams are 64×63 arcsec^2 (na) and 31.8×31.2 arcsec^2 ($r = 0$); the measured rms noise is 1.7 and 1.8 mJy beam^{-1}, respectively. The H I data cubes were corrected for primary-beam attenuation. 1 Jy beam^{-1} km s^{-1} corresponds to an H I column density of 2.8×10^{20} atoms cm^{-2} (na) and 11.2×10^{20} atoms cm^{-2} ($r = 0$).

Radio continuum maps were made using uniform weighting of the *uv* data. After CLEANing, they were restored with a synthesized beam of 6 arcsec, resulting in an rms of 0.5 mJy beam^{-1}. A low-resolution image was created using natural weighting; only the shortest 10 baselines were used. The beam size here is 76×71 arcsec^2, with an rms of 0.8 mJy beam^{-1}.

Table 2. Observing parameters.

ATCA configuration	1.5A	375
Primary-beam	33 arcmin	
Pointing position	$03^h\,59^m\,25^s$	
in α, δ (J2000)	$-67^\circ\,47'\,00'$	
Total observing time	712 min	647 min
Centre frequency	1414 MHz	
Total bandwidth	8 MHz	
Number of channels	512	
Velocity resolution	6.6 km s^{-1}	
(after Hanning smoothing)		
Calibrator flux densities:		
primary	1934–638 (14.88 Jy)	
secondary	0355–669 (0.97 Jy)	

3 RADIO CONTINUUM RESULTS

Because the overall, extended radio continuum emission of NGC 1511 was analysed by Dahlem et al. (2001), we concentrate here on the central region. Fig. 1 shows a high-resolution 20-cm radio continuum image of NGC 1511 overlaid on to *B*- and *H*-band images from Eskridge et al. (2002). We identify three maxima at α, δ (J2000) $=03^h59^m40.7^s$, $-67\hat{3}8''.8$ (SE complex), $03^h59^m36\overset{s}{.}5$, $-67^\circ38'02''.0$ (middle source) and $03^h59^m33\overset{s}{.}7$, $-67^\circ38'01''.1$ (faint western source) with approximate peak flux densities of 53, 27 and 13 mJy beam^{-1}, respectively. The SE complex corresponds to the peculiar hook, which is best seen in the *H*-band image (Eskridge et al. 2002) and the Two Micron All-Sky Survey JHKs-image (Jarrett et al. 2003). At the same location, the *B*-band image shows a chain of bright hotspots. These are young H II regions (see Lehnert & Heckman 1995) consistent with increased star formation in that part of the disc of NGC 1511. The middle source, which lies ∼6 arcsec north-east of the galaxy centre as given in Table 1, and the faint western source also appear to coincide with hotspots in the Hα image. No radio continuum emission was

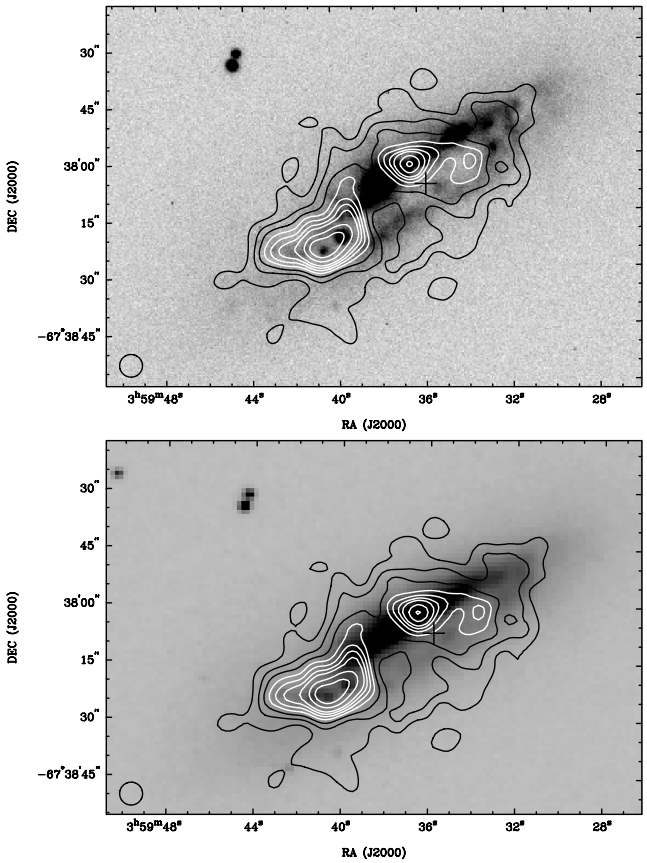

Figure 1. High-resolution 20-cm radio continuum emission of NGC 1511 overlaid on to *B*-band (top) and *H*-band (bottom) images from Eskridge et al. (2002). The contour levels are 1, 1.5, 2, 2.5, 3, 3.5, 4, 4.5, 5, 5.5, 6 and 6.5 mJy beam^{-1}. The galaxy centre (see Table 1) is marked with a cross. The synthesized beam (6 arcsec) is displayed at the bottom left corner.

detected from the companions, NGC 1511A and B, with 5σ upper limits to their flux densities of $\sim$4 mJy. We detect several background sources in the observed field; the two brightest are SUMSS J035734–674941 (30 mJy) and SUMSS J035949–680052 (68 mJy).

To estimate the star formation rate (SFR) of NGC 1511 from the 20-cm radio continuum flux density, S_{20} (Jy), we use SFR ($M_\odot yr^{-1}$) = 0.14 D^2 $S_{20\,cm}$ derived from Condon (1992) and Haarsma et al. (2000), where D is the distance in Mpc. For NGC 1511, we measure a primary-beam corrected 20-cm radio continuum flux density of 167 mJy (using the low-resolution map) and hence an SFR of $\sim$7 $M_\odot yr^{-1}$. There are indications of a faint extended halo, but our data are not sufficient to study this emission. For comparison, Dahlem et al. (2001) measure a total 20-cm radio continuum flux density of 156 $\pm$ 8 mJy. For NGC 1511A and B, we derive upper limits of SFR $<$0.2 $M_\odot yr^{-1}$.

The SFR of a galaxy can also be estimated from its far-infrared (FIR) luminosity, L_{FIR}, using SFR ($M_\odot yr^{-1}$) = 0.17 L_{FIR} (Kennicutt 1998), with L_{FIR} in units of 10^9 $L_\odot$. Using the *IRAS* 60- and 100-μm flux densities given by Sanders et al. (1995; $S_{60\,\mu m}$ = 25.7 Jy, $S_{100\,\mu m}$ = 41.3 Jy, for comparison see Table 1), we derive a FIR luminosity of 1.36 $\times$ 10^{10} $L_\odot$ for NGC 1511, which results in SFR = 2.2 $M_\odot yr^{-1}$. NGC 1511A has an infrared luminosity of 1.4–4.0 $\times$ 10^8 $L_\odot$ and SFR = 0.02–0.07 $M_\odot yr^{-1}$. No *IRAS* flux densities are available for NGC 1511B.

Following Helou, Soifer & Rowan-Robinson (1985), we calculated the parameter q, which is the logarithmic ratio of FIR to radio flux density. For NGC 1511, we find q = 2.34, consistent with the mean value of 2.3 for normal spiral galaxies (Condon 1992).

4 H I RESULTS

The H I channel maps of the NGC 1511 group are shown in Fig. 2. All three galaxies are clearly detected, covering a velocity range of 1130 to 1510 km s^{-1}. In addition, we detect a thin H I bridge between NGC 1511 and 1511B, indicating tidal interactions or a direct collision of the two galaxies. No bridge is detected towards NGC 1511A. The individual H I spectra are displayed in Fig. 3. Most noticeable is the rather narrow H I spectrum (1370–1480 km s^{-1}) of the disturbed, edge-on galaxy NGC 1511B, in contrast to the broad spectra of NGC 1511 and 1511A. We estimate the systemic velocity of NGC 1511B to be 1425 km s^{-1}, close to the Hα velocity (see Table 1). Note that Nordgren et al. (1997) find the H I spectrum of NGC 1511B peaks at 1429 km s^{-1}, in agreement with our value. Because they claim to see faint H I emission at lower velocities, they estimate v_{sys} = 1304 km s^{-1}. The H I bridge, which appears to connect the north-western edge of NGC 1511 to the western edge of NGC 1511B covers a velocity range from $\sim$1320 to 1430 km s^{-1}. Both the H I and the stellar disc of NGC 1511B are affected by the interaction. It is likely that the gas in the H I bridge was stripped from NGC 1511B by a direct collision with the outer disc of NGC 1511.

The H I distribution, the mean H I velocity field and the H I velocity dispersion of the NGC 1511 group are shown in Fig. 4. For a summary of the H I properties see Table 3.

We measure a total primary-beam corrected H I flux density of F_{HI} = 74 Jy km s^{-1} for the NGC 1511 group resulting in an H I mass of M_{HI} = 5.4 $\times$ 10^9 $M_\odot$. For NGC 1511 alone, we measure F_{HI} = 66.4 Jy km s^{-1}, which corresponds to an H I mass of 4.8 $\times$ 10^9 $M_\odot$, while the two small companions, NGC 1511A and B, have H I masses of 2.0 and 3.7 $\times$ 10^8 $M_\odot$, respectively. For a summary, see Table 3. The H I Parkes All-Sky Survey (HIPASS) Bright Galaxy Catalogue (Koribalski et al. 2004) gives the following H I properties for NGC 1511 (HIPASS J0359–67): a systemic velocity of v_{sys} = 1333 $\pm$ 5 km s^{-1}, 50 and 20 per cent velocity widths of 267 and 323 km s^{-1}, respectively, and F_{HI} = 65.9 $\pm$ 5.0 Jy km s^{-1}, i.e. M_{HI} = 4.8 ($\pm$0.3) $\times$ 10^9 $M_\odot$. The H I flux density given in HIPASS Catalogue (HICAT) (F_{HI} = 74.2 km s^{-1}; Meyer et al. 2004) was measured over a larger area (36 $\times$ 36 arcmin^2) and is consistent with our H I measurement of the whole group. This agreement indicates that very little (if any) diffuse H I emission has been filtered out by the interferometric observation, i.e. the NGC 1511 group does not contain large amounts of undetected H I gas. This is perhaps not surprising as the main interaction appears to occur between NGC 1511 and 1511B and those scales are well covered by the ATCA observations.

Previous H I measurements of NGC 1511, obtained with the 64-m Parkes telescope, include F_{HI} = 63.7 $\pm$ 6.1 Jy km s^{-1} (Reif et al. 1982), 85.3 Jy km s^{-1} (Bajaja & Martin 1985) and 73.6 Jy km s^{-1} (Mathewson & Ford 1996).

5 DISCUSSION

5.1 Signatures of galaxy interactions

Gaseous, intergalactic emission is detected between NGC 1511 and 1511B in the velocity range from $\sim$1320 to 1430 km s^{-1} (see Figs 2 and 5). It commences at the north-western side of NGC 1511 and

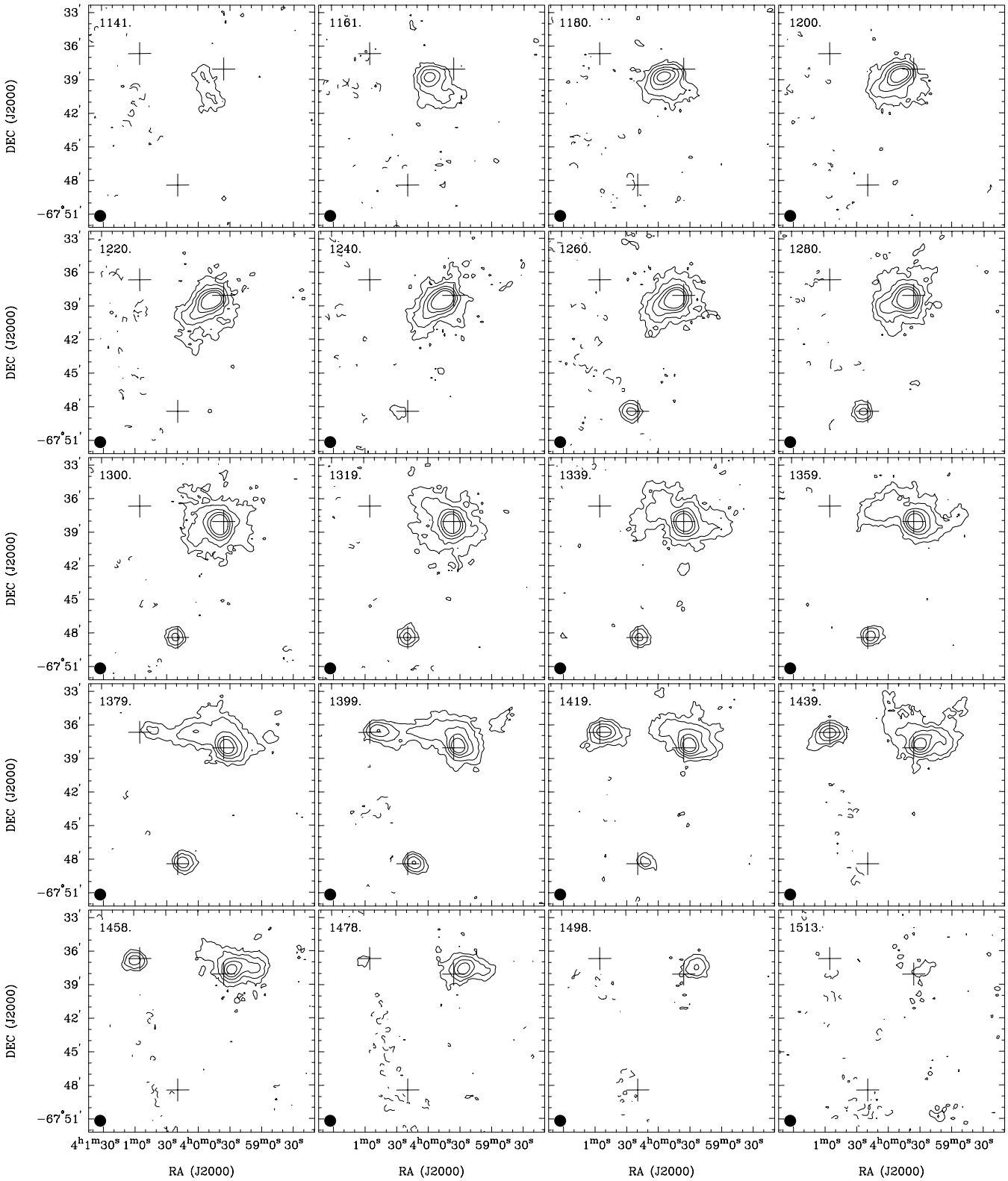

Figure 2. H I channel maps of the NGC 1511 group using natural weighting. The three galaxy centres are marked as given in Table 1. The contour levels are −3, 3, 6, 12, 20 and 30 mJy beam^{-1}. The synthesized beam (64 × 63 arcsec^2) is displayed at the bottom left corner and the heliocentric velocity of each channel at the top left.

appears to curve around to the western side of NGC 1511B, extending over a distance of at least 37 kpc. The overall bridge area contains up to ∼6 Jy km s^{-1}, corresponding to an H I mass of ∼4 × 10^8 M$_\odot$; this gas is currently attributed to either NGC 1511 or 1511B in Table 3 because, with the current data, it is impossible to exactly specify how much H I gas lies between the galaxies. No stellar counterpart to the bridge has been detected in the available optical sky surveys.

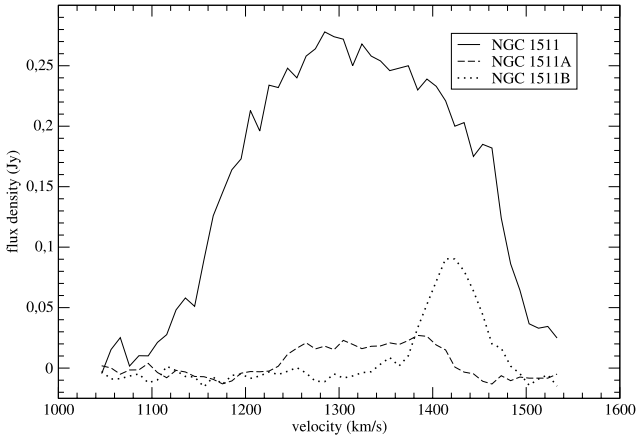

Figure 3. Integrated H I spectra of the three galaxies in the NGC 1511 group.

The stellar distribution of NGC 1511B is extremely thin and edge-on. Its main body extends 1.7 arcmin (9 kpc) along the major axis. In addition, we find a faint extension towards the west with a prominent H II region at its tip, which corresponds to the H I maximum in the 1393 km s^{-1} channel map. The H I and the stellar disc of NGC 1511B seem to be elongated and severely distorted, especially in the direction of NGC 1511. In addition, the H I velocity field of NGC 1511B does not look like that of a normal rotating spiral galaxy. The isovelocity contours are inclined with respect to the disc major axis, at an angle of $\sim$45°, and are generally irregular (see Fig. 6). The velocity dispersion stays around 17 km s^{-1} throughout the disc. It seems that the H I gas distribution of NGC 1511B has been distorted and partially stripped off by gravitational forces during the interaction/collision with its massive neighbour, NGC 1511. The dynamical mass estimate given for NGC 1511B (see Table 4) is highly uncertain as the actual rotational velocity of the galaxy is unknown.

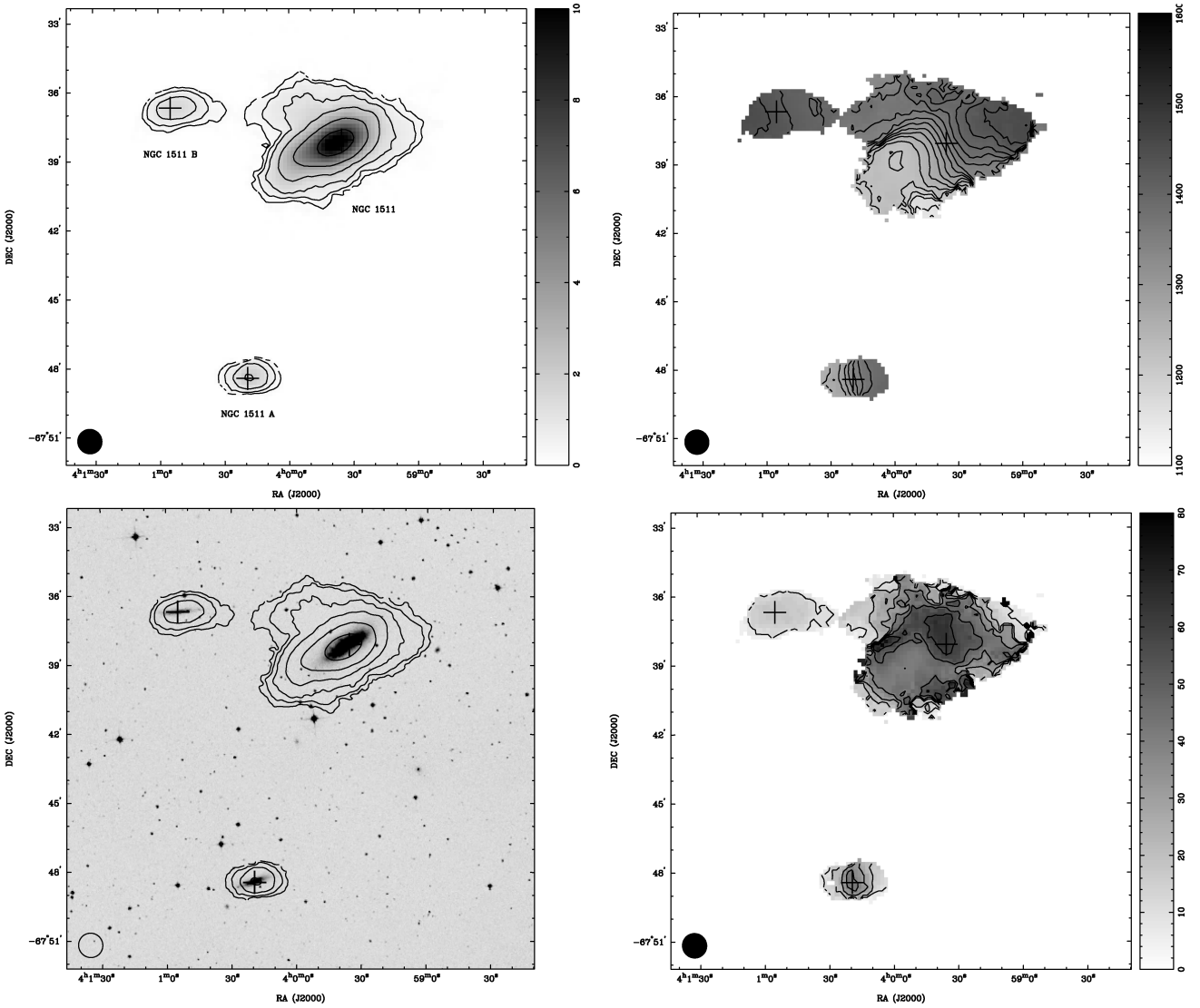

Figure 4. The H I gas dynamics of the galaxy group NGC 1511 (using natural weighting). The optical galaxy centres (see Table 1) are marked. Top left panel: H I distribution (0 moment). The contour levels are 0.25, 0.5, 1, 2, 4 and 8 Jy beam^{-1} km s^{-1} (corresponding to H I column densities of 6.9 $\times$ 10^{19} to 2.2 $\times$ 10^{21} atoms cm^{-2}). Top right: mean H I velocity field (1 moment). The contour levels range from 1160 to 1480 km s^{-1}, in steps of 20 km s^{-1}. Bottom left: H I distribution (contours) overlaid on to an optical image (grey-scale) from the Digitized Sky Survey (DSS). The contour levels are as in the top left panel. Bottom right: H I velocity dispersion (2 moment). The contour levels are 10, 20, 30, 40, 50 and 60 km s^{-1}. The synthesized beam (64 $\times$ 63 arcsec^2) is marked in the bottom left corner.

Table 3. H I properties of the galaxies and the bridge in the NGC 1511 group as measured with the Australia Telescope Compact Array (ATCA).

Object	Velocity range (km s^{-1})	$F_{\rm HI}$ (Jy km s^{-1})	$M_{\rm HI}$ (10^8 M$_\odot$)
Group	1130–1510	74	53.5
NGC 1511	1130–1510	66.4	48.0
NGC 1511A	1240–1410	2.8	2.0
NGC 1511B	1370–1480	5.1	3.7

Another most interesting feature found near NGC 1511 is a peculiar vertical ridge (∼1.5 arcmin in length) only visible in deep optical images. It is located ∼3 arcmin east of the centre of NGC 1511 and corresponds to a distinct region in the H I velocity field of NGC 1511 (see Fig. 7). While this region is peculiar with respect to the rotation of NGC 1511, it shows remarkably regular isovelocity contours perpendicular to the ridge. We tentatively conclude that what appears like a peculiar ridge actually is the stellar remnant of a tidally disrupted galaxy in the NGC 1511 group.

Bridges between galaxies, either consisting of gas only or with a stellar component, are observed in several galaxy pairs (e.g. Irwin 1994; Smith et al. 1997; Struck & Smith 2003; Koribalski & Dickey 2004). Simulations show two different mechanisms for developing bridges. Toomre & Toomre (1972) first predicted bridges to be formed by tidal forces. This process is successfully modelled by Barnes & Hernquist (1991) and Mihos & Hernquist (1996), considering an impact parameter larger than the disc radius. In this case, stars and gas are stripped out in the bridge. Struck (1997) discusses the formation of splash bridges, which are formed during a close encounter (impact parameter smaller than disc radius). Gas clouds of both galaxies collide and form a gas bridge between them, typically without any stellar counterpart. In this kind of bridge, no star formation is initially expected. The H I bridge between NGC 1511 and 1511B seems to be a splash bridge, suggesting that NGC 1511B has plunged through the outer disc of NGC 1511 during its closest encounter.

5.2 The kinematics of NGC 1511 and its companions

In the inner part of its disc, NGC 1511 shows a clear rotation pattern. By fitting all rotational parameters simultaneously for radii from 30 to 300 arcsec, we find the kinematic centre at α, δ(J2000) = $03^{\rm h}59^{\rm m}39\overset{\rm s}{.}0$, $-67^\circ38'10\overset{''}{.}0$, a systemic velocity of $v_{\rm sys} = 1333 \pm 5$ km s^{-1} and a position angle of $PA = 300^\circ \pm 2^\circ$. We note that there is a substantial offset between the optical centre of NGC 1511 as given in Table 1, the 2MASS position and the kinematic centre as determined here. Because the fit of the position angle appeared constant with radius, we fixed its value to 300°. The inclination angle was difficult to fit and we used $i = 74^\circ$ (Table 1). With the two orientation parameters fixed, we derive a rotation curve for

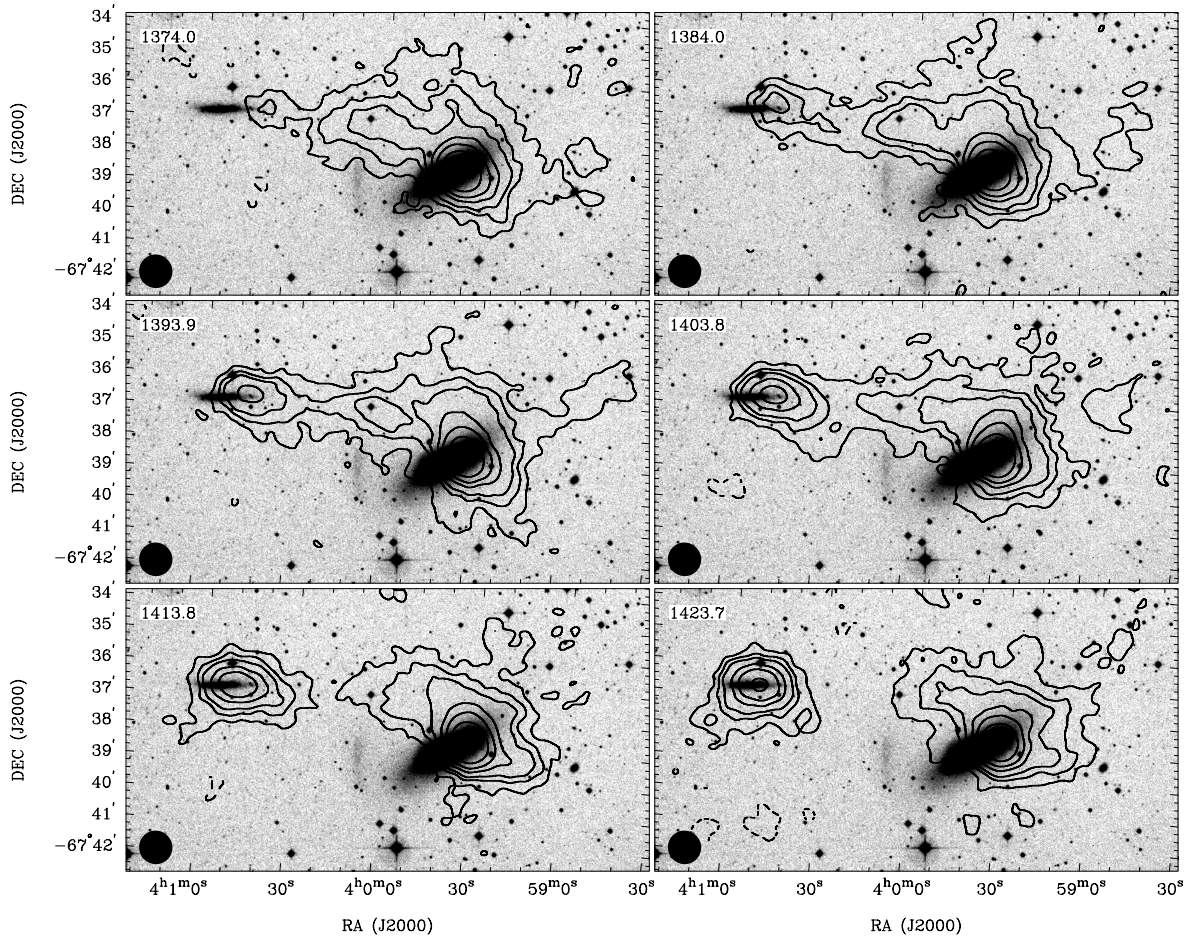

Figure 5. H I channel maps (from 1374 to 1424 km s^{-1}) overlaid on to a high contrast *B*-band image from the SuperCOSMOS Sky Survey, emphasizing the narrow bridge between the interacting galaxies NGC 1511 and 1511B. The contour levels are −3, 3, 6, 9, 15, 21 and 30 mJy beam^{-1}. The beam is displayed at the bottom left corner and the heliocentric velocity of each channel at the top left.

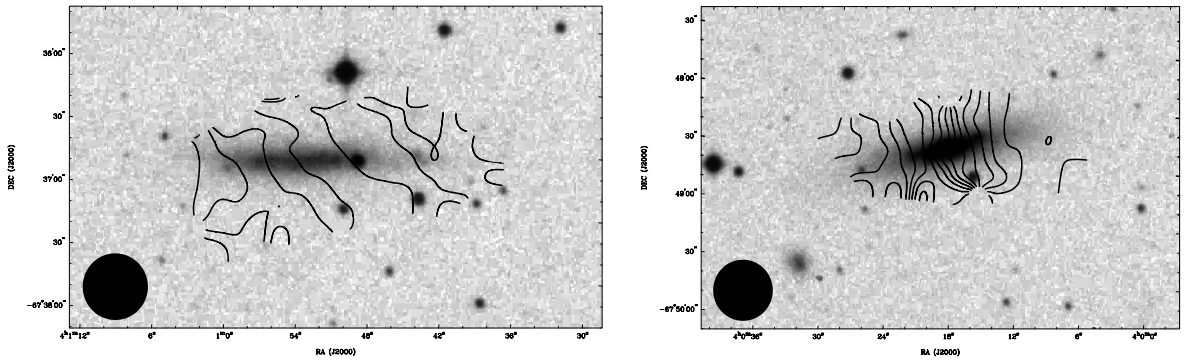

Figure 6. Mean H I velocity fields of the two companion galaxies, NGC 1511B (left) and NGC 1511A (right), and NGC 1511 (right) overlaid on to *B*-band images from the SuperCOSMOS Sky Survey. For these images, we used robust weighting ($r = 0$), resulting in a synthesized beam of 31.8×31.2 arcsec^2, to emphasize the inner disc. The contour levels range from 1400 to 1460 km s^{-1} (for NGC 1511B) and 1250 to 1400 km s^{-1} (for NGC 1511A), in steps of 10 km s^{-1}. For comparison see Fig. 4.

Table 4. Derived properties of the galaxies in the NGC 1511 triplet.

Object	$v_{\rm sys}$ (km s^{-1})	$v_{\rm rot}$ (km s^{-1})	$r_{\rm HI}$ (kpc)	$M_{\rm tot}$ (10^9 M$_\odot$)	$M_{\rm HI}/M_{\rm tot}$	$M_{\rm tot}/L_{\rm B}$	$M_{\rm HI}/L_{\rm B}$
NGC 1511	1333	130	25	98	0.07	20	1.4
NGC 1511A	1325	88	8	14	0.02	20	0.4
NGC 1511B	1425	55?	10	7	0.07	23	1.7

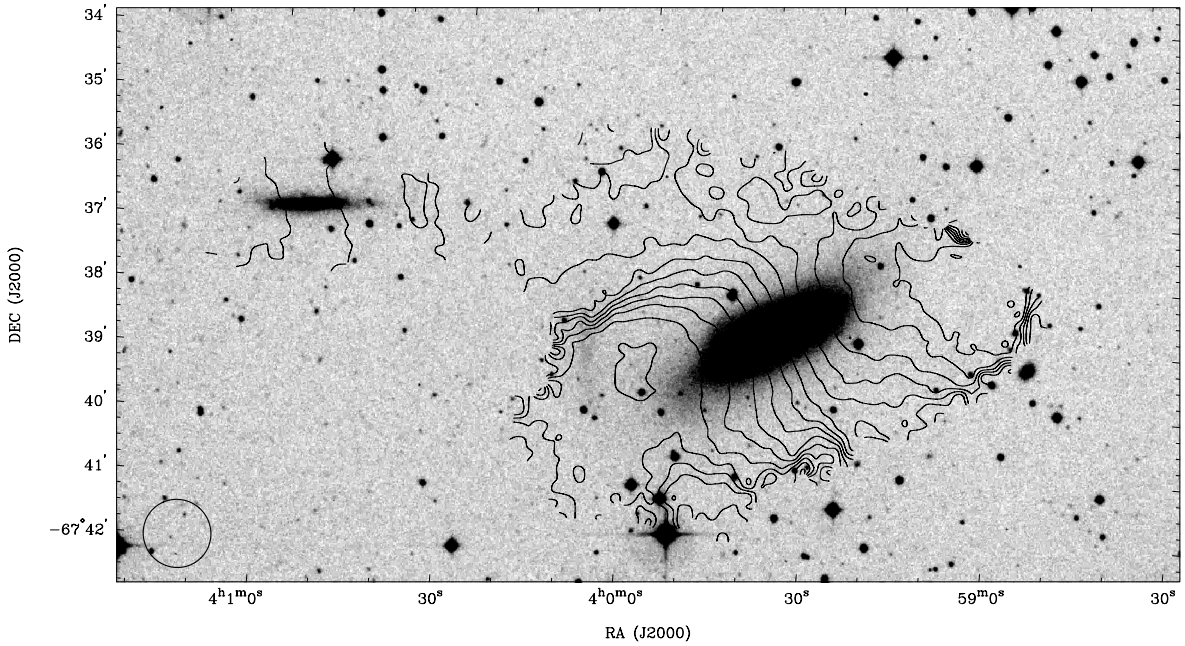

Figure 7. Mean H I velocity field of the galaxy NGC 1511 (identical to Fig. 4) overlaid on to a *B*-band image from the SuperCOSMOS Sky Survey to emphasize the gas kinematics in the region of the peculiar optical ridge. The contour levels range from 1160 to 1480 km s^{-1}, in steps of 20 km s^{-1}.

the approaching side (AS), the receding side (RS) and for both sides (BS) of NGC 1511 (see Fig. 8). While the AS of the galaxy shows a rather flat rotation curve, the RS appears slightly irregular, possibly showing the effects of interactions, which are most evident at the higher H I velocities in the system. Given a maximum H I rotation velocity of ∼130 km s^{-1} and an H I extent of ∼300 arcsec (25 kpc), we derive a dynamical mass of $\sim 10^{11}$ M$_\odot$. As a result of the low angular resolution of our H I data compared with the size of the two companion galaxies, we were not able to fit their rotation curves.

In Table 4, we list the systemic velocities, the rotation velocities and the H I radii of all three galaxies in the NGC 1511 group, as well as their dynamical masses and mass-to-light ratios. For NGC 1511A and B, we estimate $v_{\rm sys}$ as the central velocity of the H I spectrum and $v_{\rm rot}$ as the half width of each spectrum, corrected for inclination taken from Table 1.

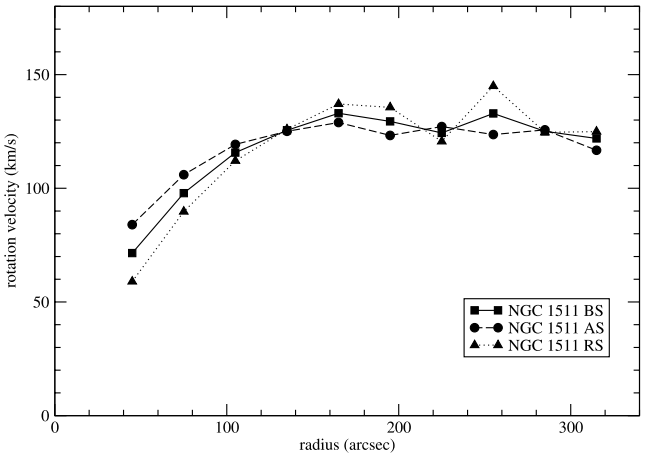

Figure 8. Rotation curve model for NGC 1511 for the approaching, receding and both sides (AS, RS and BS, respectively). For a description of the fit parameters and their uncertainties see Section 5.2.

Adding the dynamical masses of the three galaxies together results in $M_{\rm tot}$ (group) $= 1.2 \times 10^{11}\,{\rm M}_{\odot}$. For comparison, the virial mass (see Heisler, Tremaine & Bahcall 1985) of the NGC 1511 group is $\sim 4.4 \times 10^{11}\,{\rm M}_{\odot}$, a factor 3.7 larger.

The H I velocity field of NGC 1511 (Fig. 7) shows a broad distribution with an extension to the south-east towards the peculiar optical ridge. In that area, the optical image of NGC 1511 also shows peculiarities such as outflows and diffuse extended emission.

6 CONCLUSIONS

ATCA H I and 20-cm radio continuum observations of the NGC 1511 triplet reveal an H I–rich group with a striking gaseous bridge between the massive galaxy NGC 1511 and its minor companion NGC 1511B, as well as substantial star formation in the disc of NGC 1511. While the gas distribution of NGC 1511B is strongly affected by the interaction, a second, more distant companion galaxy, NGC 1511A, remains unaffected. There may have been a fourth member of the galaxy group, which now appears to be completely disrupted, leaving only the faint stellar remnant and a merging H I distribution. In the following, we briefly summarize our results.

(i) H I emission was detected from all three galaxies in the NGC 1511 triplet. Assuming a distance of 17.5 Mpc for the group, we derive H I masses of $M_{\rm HI} = 4.8 \times 10^9\,{\rm M}_{\odot}$ (NGC 1511), $2.0 \times 10^8\,{\rm M}_{\odot}$ (NGC 1511A) and $3.7 \times 10^8\,{\rm M}_{\odot}$ (NGC 1511B).

(ii) In addition, we found an H I bridge connecting NGC 1511 and 1511B with an H I mass of up to $4 \times 10^8\,{\rm M}_{\odot}$. The bridge, which was most likely formed through a close encounter of the two neighbouring galaxies, has no apparent optical counterpart. The projected distance between NGC 1511 and 1511B is $\sim$37 kpc, indicating an approximate time of $\gtrsim$200 Myr since their last collision.

(iii) The H I distribution of NGC 1511B appears to have been severely stretched and displaced by the interaction/collision with NGC 1511. It has a rather narrow H I spectrum (for an edge-on galaxy) and an unusual H I velocity field. In contrast, the more distant companion, NGC 1511A, shows no signs of interaction.

(iv) The peculiar optical ridge found to the east of NGC 1511 may be the stellar remnant of another group member, now completely disrupted by interactions with NGC 1511.

(v) For the NGC 1511 group, we derive a total H I mass of $5.4 \times 10^9\,{\rm M}_{\odot}$ ($\sim$90 per cent of which resides in NGC 1511 itself), a combined dynamical mass of $\sim 1.2 \times 10^{11}\,{\rm M}_{\odot}$ and a virial mass of $\sim 4.4 \times 10^{11}\,{\rm M}_{\odot}$.

(vi) High-resolution ATCA radio continuum data show that most of the emission is occurring in the south-eastern part of the NGC 1511 disc, coincident with a prominent chain of H II regions. We measure a total 20-cm continuum flux density of 167 mJy for NGC 1511, which corresponds to an SFR of $7\,{\rm M}_{\odot}{\rm yr}^{-1}$. Deriving the SFR from the FIR luminosity, we determine a value of $2.2\,{\rm M}_{\odot}{\rm yr}^{-1}$, resulting in a q parameter of 2.34. For the companions, NGC 1511A and B, we derive upper limits of SFR $= 0.2\,{\rm M}_{\odot}{\rm yr}^{-1}$.

ACKNOWLEDGMENTS

The observations of the NGC 1511 galaxy group were obtained with the Australia Telescope, which is funded by the Commonwealth of Australia for operations as a National Facility managed by the Commonwealth Scientific and Industrial Research Organisation (CSIRO). We acknowledge the use of the SuperCOSMOS Sky Survey. This research has made extensive use of the NASA/IPAC Extragalactic Data base (NED), which is operated by the Jet Propulsion Laboratory, Caltech, under contract with the National Aeronautics and Space Administration. The Digitized Sky Survey (DSS) was produced by the Space Telescope Science Institute (STScI) and is based on photographic data from the UK Schmidt Telescope, the Royal Observatory Edinburgh, the UK Science and Engineering Research Council and the Anglo-Australian Observatory. We thank the referee for some excellent comments.

REFERENCES

Bajaja E., Martin C., 1985, AJ, 90, 1783
Barnes J. E., Hernquist L., 1991, ApJ, 370, L65
Broeils A. H., van Woerden H., 1994, A&AS, 107, 129
Condon J. J., 1992, ARA&A, 30, 575
Dahlem M., Lazendic J. S., Haynes R. F., Ehle M., Lisenfeld U., 2001, A&A, 374, 42
Dahlem M., Ehle M., Jansen F., Heckman T. M., Weaver K. A., Strickland D. K., 2003, A&A, 403, 547
Elfhag T., Booth R. S., Höglund B., Johansson L. E. B., Sandqvist A., 1996, A&AS, 115, 439
Eskridge P. B. et al., 2002, ApJ, 143, L73
Haarsma D. B., Partridge R. B., Windhorst R. A., Richards E. A., 2000, ApJ, 544, 641
Heisler J., Tremaine S., Bahcall J. N., 1985, ApJ, 298, 8
Helou G., Soifer B. T., Rowan-Robinson M., 1985, ApJ, 298, L7
Hibbard J. E., van Gorkom J. H., Rupen M. P., Schiminovich D., 2001, in Hibbard J. E., Rupen M. P., van Gorkom J. H., eds, ASP Conf. Ser. Vol. 240, Gas and Galaxy Evolution. Astron. Soc. Pac., San Francisco, p. 659
Irwin J. A., 1994, ApJ, 429, 618
Jarrett T. H., Chester T., Cutri R., Schneider S., Huchra J. P., 2003, AJ, 125, 525
Kennicutt R. C., 1998, ARA&A, 36, 189
Kewley L. J., Heisler C. A., Dopita M. A., Sutherland R., Norris R. P., Reynolds J., Lumsden S., 2000, ApJ, 530, 704
Koribalski B., 1996, in Buta R., Crocker D. A., Elmegreen B. G., eds, IAU Coll. 117, ASP Conf. Ser. Vol. 91, Barred Galaxies. Astron. Soc. Pac., San Francisco, p. 172
Koribalski B., Dickey J. M., 2004, MNRAS, 348, 1255
Koribalski B., Dahlem M., Mebold U., Brinks E., 1993, A&A, 268, 14
Koribalski B. et al., 2004, AJ, 128, 16
Lauberts A., 1982, ESO/Uppsala survey of the ESO(B) atlas(ESO-LV). Garching, European Southern Observatory (ESO)
Lehnert M. D., Heckman T. M., 1995, ApJ, 97, L89
Mathewson D. S., Ford V. L., 1996, ApJ, 107, L97

Meyer M. J. et al., 2004, MNRAS, 350, 1195
Mihos J. C., Hernquist L. 1996, ApJ, 464, 641
Moshir M. et al., 1990, BAAS, 22, 1325
Nordgren T. E., Chengalur J. N., Salpeter E. E., Terzian Y., 1997, AJ, 114, 913
Reif K., Mebold U., Goss W. M., van Woerden H., Siegman B., 1982, A&A, 50, 451
Salpeter E. E., Hoffman G. L., 1996, ApJ, 465, 595
Sandage A., Bedke J., 1994, The Carnegie Atlas of Galaxies. Carnegie Institution of Washington, Washington D.C.
Sanders D. B., Egami E., Lipari S., Mirabel I. F., Soifer B. T., 1995, AJ, 110, 1993
Schlegel D. J., Finkbeiner D. P., Davis M., 1998, ApJ, 500, 525
Sekiguchi K., Wolstencroft R., 1993, MNRAS, 263, 349
Smith B. J., Struck C., Pogge R. W., 1997, ApJ, 483, 766
Strong A. W. et al., 1988, A&A, 207, 1
Struck C., 1997, ApJ, 113, L269
Struck C., Smith B. J., 2003, ApJ, 589, 157
Thornley M. S., Schreiber N. M. F., Lutz D., Genzel R., Spoon H. W. W., Kunze D., Sternberg A., 2000, ApJ, 539, 641
Toomre A., Toomre J., 1972, ApJ, 178, 623
de Vaucouleurs G., de Vaucouleurs A., Corwin H. G., Jr, Buta R. J., Paturel G., Fouqué P., 1991, Third Reference Catalogue of Bright Galaxies. Springer Verlag, New York (RC3)
Yun M. S., Ho P. T. P., Lo K. Y., 1994, Nat, 372, 530

This paper has been typeset from a TEX/LATEX file prepared by the author.